https://doi.org/10.5194/nhess-2019-175
Preprint. Discussion started: 12 August 2019

Natural Hazards and Earth System Sciences
Discussions

Establishment and characteristics analysis of a crop-drought vulnerability curve: a case study of European winter wheat

Yanshen Wu[1], Hao Guo[1], Anyu Zhang[1], Jing'ai Wang[1,2]

[1]School of Geography, Faculty of Geographical Science, Beijing Normal University, Beijing 100875, China;
[2]Key Laboratory of Environmental Change and Natural Disaster, MOE, Beijing Normal University, Beijing 100875, China

Correspondence to: Jing'ai Wang（jwang@bnu.edu.cn)

Abstract. As an essential component of drought risk, crop-drought vulnerability refers to the degree of the adverse response of a crop to a drought event. Different drought intensities and environments can cause significant differences in crop yield losses. Therefore, quantifying the drought vulnerability and then identifying its spatial distribution pattern will contribute to understanding vulnerability and the development of risk-reduction strategies. We select the European winter wheat growing area as the study area and 0.5°×0.5° grids as the basic assessment units. Winter wheat drought vulnerability curves are established based on the Erosion-Productivity Impact Calculator model simulation. Their loss transmutation and loss extent characteristics are quantitatively analysed by the key points and cumulative loss rate, respectively, and are then synthetically identified VIA K-means clustering. The results show the following. (1) The regional yield loss rate starts to rapidly increase from 0.13 when the drought index reaches 0.18 and then converts to a relatively stable stage with the value of 0.74 when the drought index reaches 0.66. (2) The stage transitions of the vulnerability curve lag in the southern mountain area, indicating a stronger tolerance to drought in the system, in contrast to the Pod Plain. (3) According to the loss characteristics during the initial, development and attenuation stages, the vulnerability curves can be divided into five clusters, namely, Low-Low-Low, Low-Low-Medium, Medium-Medium-Medium, High-High-High and Low-Medium-High loss types, corresponding to the spatial distribution from low latitude to high latitude and from mountain to plain. It is recommended to improve the integrated mitigation capability in the Medium-Medium-Medium and High-High-High loss type areas and to develop the ability to mitigate droughts in the 0.3-0.6 intensity range, as non-engineering measures for the droughts greater than 0.6 intensity in Low-Medium-High loss type areas.

1 Introduction

Drought is a widespread natural disaster causing the largest agricultural losses in the world. More than one-half of the earth is susceptible to drought, including nearly all of the major agricultural areas (Kogan, 1997). Under the context of climate change and globalisation, drought will pose a threat to future food security. How to assess and manage agricultural drought risks has become a focus of the world (Reid et al., 2006;Li et al., 2009;Mishra and Singh, 2010). As vulnerability is a key factor in determining risk, drought vulnerability assessment is an important foundation for drought risk assessment and management

https://doi.org/10.5194/nhess-2019-175
Preprint. Discussion started: 12 August 2019

Natural Hazards and Earth System Sciences
Discussions

(Xingming et al., 2015;Knutson C, 1998).

Crop drought vulnerability assessment focuses on crops, particularly the biophysical factors closely related to crop growth processes (J et al., 2017;González Tánago et al., 2015). Affected by factors such as the natural environment and crop variety, there are regional differences in crop drought vulnerability (IPCC, 2012, 2014). Therefore, based on a quantitative assessment, analysing and mapping their characteristics can help identify the vulnerability distribution and local mitigation-oriented drought management (Wilhelmi and Wilhite, 2002).

The commonly used crop drought vulnerability assessment methods mainly include the vulnerability index and vulnerability curve methods (Yuan-yuan et al., 2014;Jayanthi et al., 2014). The vulnerability index method identifies vulnerability indicators, determines their weights and then calculates a comprehensive value, visualising through thematic maps (Jain et al., 2014;Huang et al., 2012;Pandey et al., 2010). The indicators commonly include climate, topography, watershed location, soil, and water resource accessibility (González Tánago et al., 2015). This method can express the relative vulnerability level and the relative contribution of indicators in different regions, providing decision makers with potential means to reduce disasters (Wilhelmi and Wilhite, 2002). However, the exploration of the disaster-causing mechanism is not sufficiently comprehensive, and it is impossible to quantitatively predict losses. In addition, indicator selection and weight determination during the evaluation process have a certain subjectivity and uncertainty (Jianjun et al., 2010;Simelton et al., 2009).

The vulnerability curve method aims to quantify the crop yield response to different drought intensities. Rainfall anomalies, Standardized Precipitation Index, water stress and other indicators are often used to characterise drought intensity, yield or yield loss rate to characterise crop yield response (Yao and Jing'ai, 2012;Todisco et al., 2012;Yuan-yuan et al., 2014). The data are mainly from observation, statistics or crop model simulation. Crop model simulations are based on the crop growth and development mechanism, using mathematical physics methods and computer technology to quantitatively describe the crop growth and yield formation process in specific environments, which can solve the problem of insufficient samples or limited precision in observational or statistical data to some extent (Palosuo et al., 2011;Challinor et al., 2009). This method can provide ideas for the study of disaster-causing mechanisms and help to improve risk prediction (Papathoma-Köhle, 2016). However, because the curve is infinite dimensional data (James and Sugar, 2003), it is difficult to directly express the vulnerability and analyse the regional differences. Therefore, exploring the methods of key information mining and spatial analysis for the crop drought vulnerability curve is beneficial to improve the existing research deficiencies, which can not only quantify regional drought vulnerability based on the disaster-causing mechanism but also convey vulnerability information to decision makers from a risk visualisation perspective.

As wheat is one of the three major grain crops in the world, we select the main wheat producing area, the European winter wheat growing area, as the research area, using the $0.5° \times 0.5°$ grid as the basic assessment unit. The vulnerability curve of winter wheat drought was established based on Erosion-Productivity Impact Calculator model (EPIC) simulation. Then, the loss extent and loss variation characteristics of the vulnerability curve are extracted to analyse the vulnerability characteristics to drought in various areas. By clustering the curve shapes, areas with similar vulnerability characteristics are identified for exploring their environment and providing scientific guidance regarding the

https://doi.org/10.5194/nhess-2019-175
Preprint. Discussion started: 12 August 2019

Natural Hazards and Earth System Sciences
Discussions

development of regional drought mitigation strategies.

2 Data and methods

2.1 Basic concept

Crop drought vulnerability curve is a function of the relationship between drought intensity and loss. In theory, this function is monotonously increasing and non-linear, that is, the loss gradually increases with the increase in drought intensity (the first derivative of the curve is always greater than 0), and the growth rate of loss is phased. Restricted by ecosystem resistance, drought usually begins during the invisible accumulation period, then enters a rapid development period, and, finally, a stable end period (Chen et al., 2015). Therefore, the drought vulnerability curve should be S-shaped and can be divided into three stages as follows (Wang et al., 2013;Kucharavy and De Guio, 2011): (1) initial stage, corresponding to low drought intensity and slight loss, during which there is slow loss growth acceleration; (2) development stage, corresponding to moderate drought intensity and a rapid increase in loss, during which the loss growth rate continues to increase to reach a peak and then quickly falls; and (3) attenuation stage, corresponding to high drought intensity and stable high loss, during which the loss growth rate slowly decays (Fig. 1).

In different environments, the drought vulnerability curve presents different shapes (Yue et al., 2015;Guo et al., 2016;Wang et al., 2013) and the core lies in the difference in loss extent and loss variation (Wang et al., 2013;Hu et al., 2012;Gottschalk and Dunn, 2005). Therefore, the key points of the curve—the turning point of the stages (the third order is 0) and the turning point of the increasing speed (the second order is 0) are used to describe the loss variation characteristics, the cumulative loss to the loss extent characteristics, and the morphological classification to the integrated description.

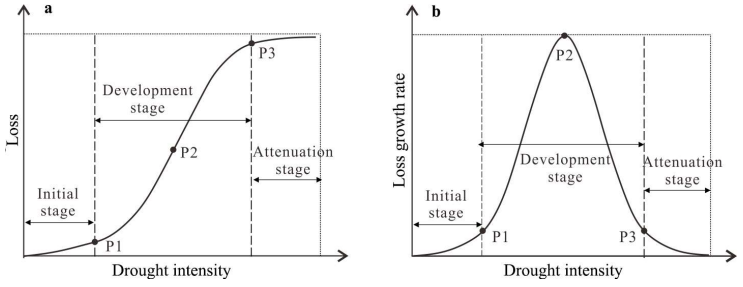

Figure 1: The relationship between drought intensity and (a) loss and (b) loss growth rate as shown by the S-shape drought vulnerability curve.

2.2 Database construction

The study area is the European wheat harvested area provided by the Center for Sustainability and the Global Environment, University of Wisconsin-Madison (Monfreda et al., 2008), and further screened by the wheat planting habit distribution map of CIMMYT (Lantican et al., 2005) for winter wheat distribution. Distributed in the range of 10° W-50° E and 42° N-59° N, this area is one of the world's major wheat-producing areas.

The EPIC model is used to simulate the growth process of winter wheat, which can simulate the crop

https://doi.org/10.5194/nhess-2019-175
Preprint. Discussion started: 12 August 2019

Natural Hazards and Earth System Sciences
Discussions

growth process and crop yield in a variety of climatic, environmental and management conditions with high precision, being widely used in many countries and regions (Zhi-qiang et al., 2008;Williams et al., 1984). It's inputs include topography, soil, meteorological, and field management data (Table 1). The soil data in this study are provided by the International Soil Reference and Information Centre (Batjes, 2012), including soil type distribution raster maps and soil physical and chemical properties lookup tables (soil bulk density, soil water content, grit content, clay content, organic carbon content, pH, etc.). The daily meteorological data are derived from HadGEM2-ES model data (Hempel et al., 2013) from 2000 to 2004, which are based on meteorological observations including solar radiation, maximum temperature, minimum temperature, average temperature, precipitation, relative humidity and average wind speed. All the original input data are processed onto 0.5° × 0.5° grids, which are the basic units for the yield simulation and vulnerability assessment.

Table 1: Basic database

Category	Name	Source	Spatial resolution
Distribution range data	Harvested area of wheat	Sustainability and the Global Environment, University of Wisconsin-Madison (Monfreda et al., 2008)	5′×5′
	Distribution of wheat planting habit	CIMMYT (Lantican et al., 2005)	Site unit
Environmental data	DEM	United States Geological Survey (1996)	0.5′×0.5′
	Slope	Food and Agriculture Organization of the United Nations / International Institute for Applied Systems Analysis (2000)	5′×5′
	Soil	International Soil Reference and Information Centre (Batjes, 2012)	5′×5′
	Historical daily meteorological data (2000~2004)	German Federal Ministry of Education and Research: the ISIMIP Fast Track project (Hempel et al., 2013)	0.5°×0.5°
Management data	Growth period of winter wheat	University of Wisconsin-Madison Sustainability and the Global Environment (Sacks et al., 2010)	0.5°×0.5°
	Irrigation	OKI Laboratory, University of Tokyo (Oki, 2002)	0.5°×0.5°
	Fertiliser	Land Use and the Global Environment (Potter et al., 2010)	0.5°×0.5°
Statistical yield data	Statistical yield for calibration (2000)	Food and Agriculture Organization of the United Nations (http://faostat.fao.org)	National（regional）unit
	Statistical yield for verification (2001~2004)		

The statistical yield data are not required for EPIC model input but for the localisation of crop parameters

https://doi.org/10.5194/nhess-2019-175
Preprint. Discussion started: 12 August 2019

Natural Hazards and Earth System Sciences
Discussions
Open Access
EGU

in the model and accuracy verification of simulated yields. They are derived from the Food and Agriculture Organization (FAO) and are country-based statistics. We use statistical yields of 2000 for model localisation, and yields of 2001-2004 for accuracy verification, to match with the years of meteorological data.

2.3 Research method

This study consists of the following three parts. (1) Calibrate the EPIC model; localise critical crop parameters in the model to improve the simulation accuracy at different locations. (2) Construct the winter wheat drought vulnerability curves based on the calibrated EPIC model simulation. For each grid unit, define series water supply scenario data and input them into the calibrated EPIC model to generate water stress and yield scenario values, thereby calculating the disaster intensity and yield loss rate, and construct a vulnerability curve. (3) Analyse the characteristics of the vulnerability curves. Extract their loss extent and loss variation characteristics and cluster morphologically similar curves, and then perform spatial analysis (Fig. 2).

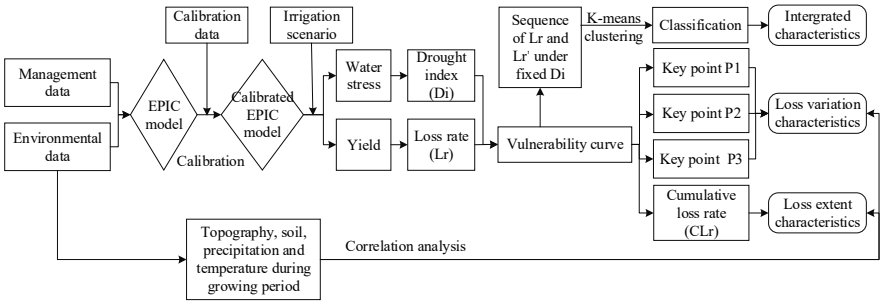

Figure 2: Basic research framework.

2.3.1 Calibration and accuracy verification of the EPIC model

The calibration method refers to the research of Guo et al. (2016). Four key parameters of WA (biomass-energy ratio), HI (harvest index), DLMA (maximum potential leaf area index), and DLAI (fraction of the growing season when the leaf area decreases) are selected for calibration (Barros et al., 2005;Wang and Li, 2010;Wang et al., 2011) .

In view of the model calibration cost, we consider that the grid units in the same country are homogeneous in the winter wheat variety, that is, they have the same set of crop parameters, which is acceptable for European countries with not large national land areas. Therefore, for all grid units within each country, the default value of the crop parameters in the EPIC model is taken as the initial value, and the actual geographical environmental, field management and meteorological data of 2000 are input to obtain the simulated yields of 2000. Then, the root mean square error (RMSE) between them and the statistical yields of 2000 are calculated. Next, we adjust the four key parameters on these grid units for another round of yield simulation and RMSE calculation. The smaller of the two RMSE values determines the following parameters adjustment direction. The parameters adjustment, yield simulation and RMSE calculation will continue in this manner until the last RMSE is less than the threshold or the number of simulations exceeds the threshold, then the adjustment work is completed.

https://doi.org/10.5194/nhess-2019-175
Preprint. Discussion started: 12 August 2019

Natural Hazards and Earth System Sciences
Discussions

The goal of EPIC model calibration is to make the simulation yield as near as possible to the statistical yield, which is also the criterion for the model accuracy. Thus, to evaluate model calibration results, we generate the simulated yields for 2001-2004 based on the calibrated EPIC model and calculate the national average simulated yields to compare to the statistical yields.

2.3.2 Vulnerability curve construction based on the calibrated EPIC model

(1) Generation of water stress and yields under different irrigation scenarios

After parameter localisation, the EPIC model can be used to simulate the winter wheat yields under different drought scenarios, providing samples of water stress (WS) and yields for the construction of vulnerability curves to drought.

To eliminate the impact of other factors on yields, we maintain the meteorological data, growth period and fertiliser addition rate constant and control the water supply condition by setting 20 irrigation scenarios for each grid evaluation unit, in which the irrigation amount uniformly increases from 0 to the optimum (the maximum irrigation amount without water stress). The optimal value is determined by pre-testing. Consequently, we obtain the outputs of 20 groups of WS and yield.

(2) Calculation of drought index and yield loss rate index

WS is an index in the EPIC model that reflects the relationship between water supply and crop water demand. The larger the value is, the more serious the water shortage will be. We normalise it to obtain the drought index (Di) as follows (Eq. (1), (2)), which can reflect both water stress intensity and stress duration:

$$Di_i = \frac{HI_i}{\max(HI)} \ , \quad (1)$$

$$HI_i = \sum_{d=1}^{n}(WS_k) \ , \quad (2)$$

where Di_i is the drought index of a grid unit under the irrigation scenario i, ranging from 0-1; HI_i is the cumulative value of water stress during the growth period under this scenario; max(HI) is the maximum value of HI_i under all irrigation scenarios; WS_k is the water stress value on day k of the growth period; and n is the number of days affected by water stress during the growth period.

The yield loss rate (Lr) is used to express the response of the yield to drought effects, calculated following Eq. (3):

$$Lr_i = \frac{\max(y)-y_i}{\max(y)} \ , \quad (3)$$

where Lr_i is the yield loss rate of a grid unit under irrigation scenario i, y_i is the yield under this scenario and max(y) is the maximum yield under the optimal irrigation scenario.

(3) Fitting of drought vulnerability curves

The aforementioned Di - Lr samples were fitted by a logistical curve to obtain the vulnerability curve on each grid unit as follows (Eq. (4)):

$$\mathrm{Lr} = \frac{\mathrm{a}}{1+\mathrm{b}\times e^{c\times Di}} + d \ , \quad (4)$$

where a, b, c, and d are constant parameters.

2.3.3 Feature extraction and spatial analysis of vulnerability curves

(1) Identification of key points

https://doi.org/10.5194/nhess-2019-175
Preprint. Discussion started: 12 August 2019

Natural Hazards and Earth System Sciences
Discussions

According to the analysis in Section 2.1, taking the derivative of Eq. (4), and setting the second and third derivatives equal to 0, the coordinates of the key points can be obtained to characterise the phase change of the vulnerability curve (Table 2).

Table 2: Key point coordinates of the vulnerability curve

	The starting point of rapid loss growth (P1)	The inflection point of rapid loss growth (P2)	The end point of rapid loss growth (P3)
Di	$-\frac{\ln(2-\sqrt{3})b}{c}$	$-\frac{\ln b}{c}$	$-\frac{\ln(2+\sqrt{3})b}{c}$
Lr	$\frac{(3-\sqrt{3})a}{6}+d$	$\frac{a}{2}+d$	$\frac{(3+\sqrt{3})a}{6}+d$

(2) Calculation of cumulative loss rate

The cumulative loss rate (CLr) is obtained by the integral of Equation 4 on the Di interval of [0,1] for describing the overall vulnerability. All CLr values are divided into five levels by natural breakpoint method: extremely low, low, moderate, high, and extremely high.

(3) Clustering of vulnerability curves

To identify the morphological characteristics of the vulnerability curves, the curves are divided into some categories by clustering. The first step is to filter the infinite dimensional curve data to a finite set of representative parameters (James and Sugar, 2003). A set of Lr and Lr' under the fixed Di value is selected to preserve both the loss extent and variation characteristics (Di=0.2, 0.4, 0.6, and 0.8, when Di=0 or 1, there is little difference in the value of Lr and Lr' between the curves). The 8 elements are separately normalised following Eq. (5) for the second step of clustering. We use the K-means clustering method to compare the distance or dissimilarity between the curves (Jacques and Preda, 2014). After clustering, the further category vulnerability curves are fitted by the Di-Lr samples of the corresponding grid vulnerability curves.

$$N(Lr_{Di=x})_t = \frac{(Lr_{Di=x})_t}{\mathrm{SD}(Lr_{Di=x})}\ , \quad (5)$$

where $(\mathrm{Lr_{Di=x}})_t$ is the value of Lr (Lr') when Di=x for the vulnerability curve t, and x=0.2, 0.4, 0.6, and 0.8; $\mathrm{SD}(\mathrm{Lr_{Di=x}})$ is the standard deviation of Lr (Lr') when Di=x for all vulnerability curves; and $\mathrm{N}(\mathrm{Lr_{Di=x}})_t$ is the normalised value.

3 Results and analysis

3.1 Verification of EPIC model simulation results

From the simulation results of the country (region) winter wheat yield from 2001 to 2004, the simulated yields are slightly lower than the statistical yields. However, there is a high degree of consistency between the two (Fig. 3). The regression equation has an R^2 between 0.89 and 0.93 and passes the test with a confidence of 0.01, indicating that the EPIC model works well in various regions and during various years.

https://doi.org/10.5194/nhess-2019-175
Preprint. Discussion started: 12 August 2019

Natural Hazards and Earth System Sciences
Discussions

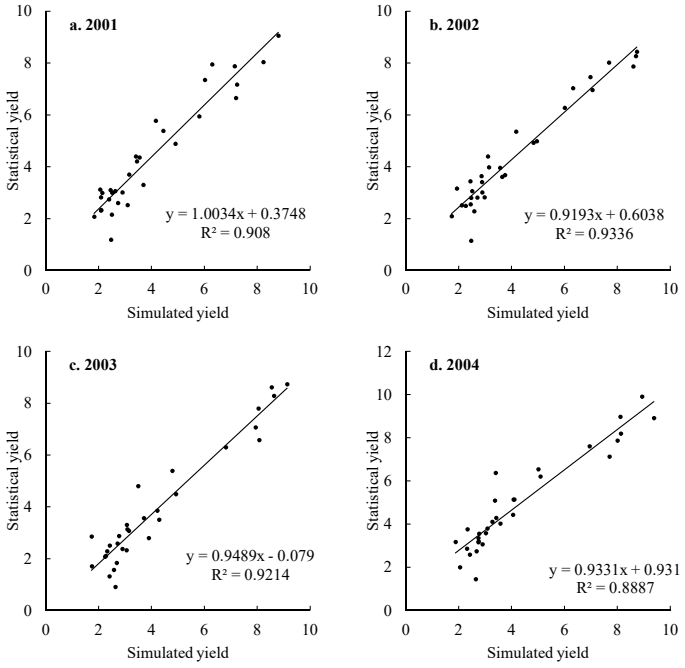

Figure 3: Regression relationship between statistical winter wheat yield and simulated yield based on country units during (a) 2001; (b) 2002; (c) 2003; and (d) 2004.

3.2 European winter wheat drought vulnerability curves and characteristics analysis

3.2.1 Winter wheat drought vulnerability curves

Figure 4a shows the winter wheat drought vulnerability curves of the 2010 grid assessment unit in Europe. Their R^2 are greater than 0.94, indicating a high overall goodness of fit. They are quite different in morphology and can be classified into several types via curve clustering (Appendix A).

The regional starting point, inflection point and end point of the rapid loss growth is corresponding to a Di of 0.27, 0.47 and 0.68 and a Lr of 0.17, 0.43 and 0.75 (Fig. 4b), respectively. For most grids, the Di at three key points is mainly distributed between 0.15-0.55, 0.35-0.7 and 0.4-0.8 and the Lr between 0.1-0.2, 0.4-0.5 and 0.7-0.8, respectively, with a relatively insignificant difference. Therefore, the Di of key points can be used to compare the difference in the stage transitions of the vulnerability curve. The larger the Di, the later the qualitative change of Lr, and the greater the tolerance to drought disturbance.

https://doi.org/10.5194/nhess-2019-175
Preprint. Discussion started: 12 August 2019

Natural Hazards and Earth System Sciences
Discussions
Open Access
EGU

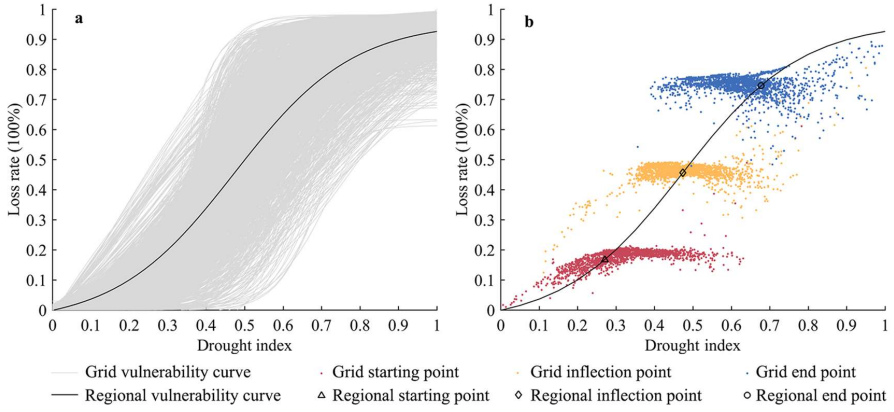

Figure 4: Distribution of (a) regional and grid vulnerability curves and (b) their key points. The regional vulnerability curve is fitted by all drought index -loss rate sample data in the region.

3.2.2 Spatial distribution of characteristic value

In terms of spatial distribution, the Di at key points to the south are higher than that to the north (Fig. 5). In the southern areas, the Di at the starting points, inflection points and end points, respectively, reach 0.4-0.5, 0.5-0.7 and greater than 0.7. The stage transitions of Lr are lagging, and the tolerance to drought disturbance is higher. In the north-central areas, the Di are respectively concentrated at less than 0.2, 0.3-0.5 and 0.5-0.7, respectively, the stages of Lr change earlier and the tolerance to drought disturbance is weaker. In the northeast, the Di at the start and end points is within the range of 0.2-0.4 and 0.4-0.6, respectively, indicating that the Lr has drastically changed during short development stages, when the areas are particularly susceptive to drought.

The CLr representing the total vulnerability shows an opposite distribution of low in the south and high in the north. Though both the north-central areas and the northeast areas have extremely high CLr values, the loss rate stages in the two areas are different. The CLr integrates the characteristics of the key points, but shows information loss in the characteristics of the loss rate transitions.

https://doi.org/10.5194/nhess-2019-175
Preprint. Discussion started: 12 August 2019

Natural Hazards and Earth System Sciences
Discussions
Open Access
EGU

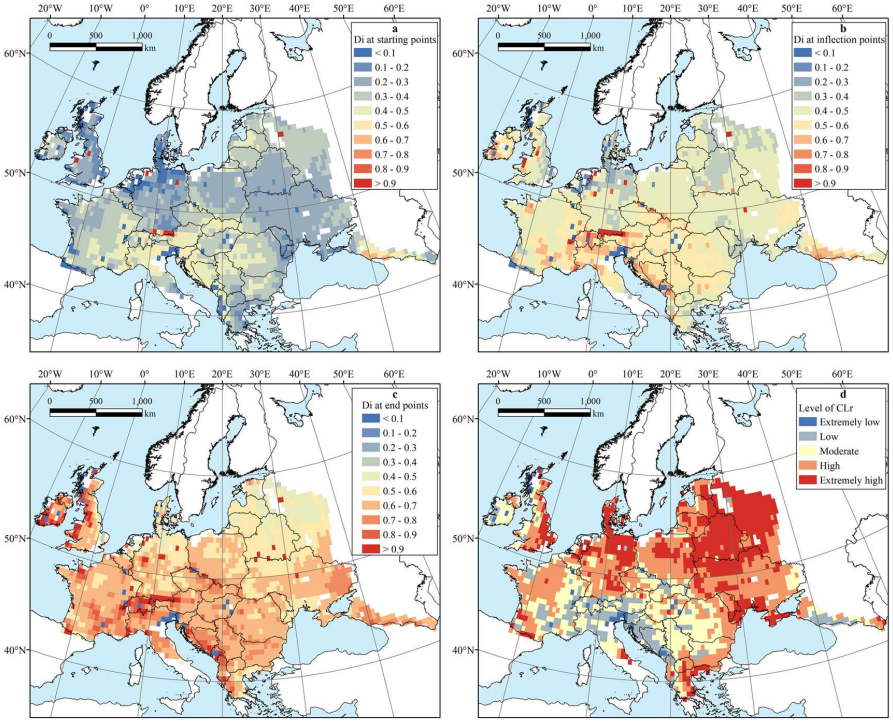

Figure 5: Spatial distributions of drought index (Di) at the (a) starting points, (b) inflection points and (c) end points, and (d) spatial distribution of level of the cumulative loss rate (CLr) of vulnerability curves.

3.3 Categories of winter wheat drought vulnerability curves

Based on the characteristics of loss extent and variation, the winter wheat vulnerability curves to drought in Europe can be divided into five types for a relatively uniform distribution, such that the results are not over-concentrated or over-classified (Appendix B). Comparing to the regional loss characteristics during the initial, development and attenuation stages, these types of vulnerability curves are defined as Low-Low-Low (L-L-L), Low-Low-Medium (L-L-M), Medium-Medium-Medium (M-M-M), High-High-High (H-H-H) and Low-Medium-High (L-M-H) loss-type vulnerability curves (Fig. 6).

The Lr of the L-L-L loss-type vulnerability curve is lower than the regional level under the same Di, and the category CLr is only 0.33, which is the lowest value of the five category vulnerability curves (Appendix C). This type of vulnerability curve is mainly distributed in mountain areas such as the Alps and the Dinara and Caucasus mountains, accounting for 10.0 % of the winter wheat planting area in Europe.

The L-L-M loss-type vulnerability curves have a relatively low loss rate and are susceptible to drought within the range of 0.4-0.7. When the Di reaches approximately 0.4, the loss rates begin to rapidly increase; when the Di values are greater than 0.6-0.7, the loss rates are near the regional level. The category CLr is 0.42. It is mainly found in the Danube river basins, including hilly areas and plains, accounting for 20.4 % of the winter wheat planting area in Europe.

The M-M-M loss-type vulnerability curves are near the regional vulnerability curve with a category CLr

https://doi.org/10.5194/nhess-2019-175
Preprint. Discussion started: 12 August 2019

Natural Hazards and Earth System Sciences
Discussions
Open Access
EGU

of 0.50, and mainly occur in the Western European Plains, the Pod Plains, Donets Ridge and surrounding highlands and lowlands. They have the widest distribution accounting for 33.9 % of the winter wheat planting area in Europe.

The Lr of the H-H-H loss-type vulnerability curve is higher than the regional level, and the category CLr reaches up to 0.57. This loss type is concentrated in patches on the Pod Plain, Polesi and in lowland areas along the Black Sea and Eastern Great Britain, at approximately the same latitude zone as that of the M-M-M loss-type, and it accounts for 23.4 % of the winter wheat planting area in Europe.

The L-M-H loss-type vulnerability curves show high susceptibility to drought in the range of 0.3-0.6, where the loss rate rapidly increases and reaches the regional level with the increase in Di. When Di values are greater than 0.6 and continue to increase, the loss rates maintain relatively stable high values; when Di values are less than 0.3, the yield losses are slight. The category CLr is 0.53. These curves are mainly distributed on the east European plain, accounting for 12.2 % of the winter wheat planting area in Europe.

On the whole, the spatial distributions of the five types of vulnerability curves are obviously latitudinal and consistent with the geographical pattern of Europe, where plains and mountains mostly extend from the east to the west in the mainland and extend from north to south in the British Isles. From south to north, and from mountain to plain, the vulnerability curves transition from concave to convex, and the CLrs show an upward trend, indicating increasing vulnerability. The heat difference at different latitudes and the water and heat difference at different altitudes may be the root cause of the type distribution.

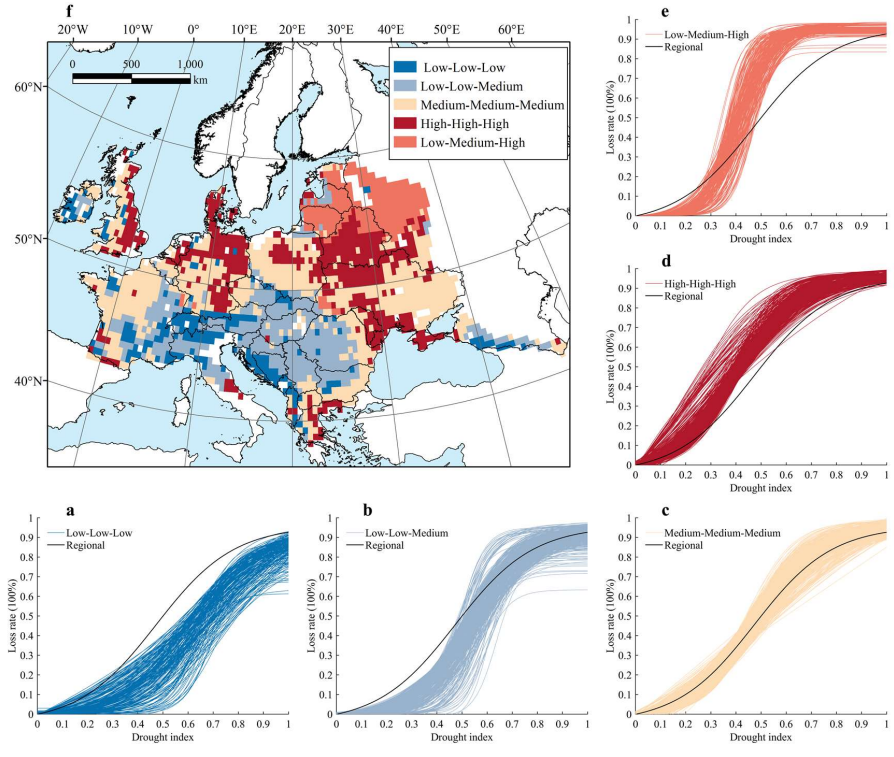

https://doi.org/10.5194/nhess-2019-175
Preprint. Discussion started: 12 August 2019

Figure 6: Five types of European winter wheat vulnerability curves to drought: (a) Low-Low-Low, (b) Low-Low-Medium, (c) Medium-Medium-Medium, (d) High-High-High and (e) Low-Medium-High loss type vulnerability curves, and (f) their spatial distributions.

4 Discussion

4.1 Relationship between vulnerability characteristics and environmental variables

To further explore the relationship between the vulnerability characteristics parameter distribution and environmental variables, Spearman correlation analysis is performed between the vulnerability characteristics parameters (Di_1, Di_2, Di_3, and CLr) and environmental variables (elevation, slope, soil sand content, precipitation during growth period, average temperature during growth period, and relative humidity during growth period). The results all passed the significance test at the level of 0.01 (Table 3). The Di_1 value is positively correlated with relative humidity and elevation, and the correlation coefficient is 0.41 and 0.40, respectively. That is, in areas with high relative humidity or altitude, only when the drought develops to a rather serious extent does it begin to have a significant impact on winter wheat yield. The L-L-L, L-L-M and L-M-H loss-type areas with high Di_1 values have the characteristics of high elevation or high relative humidity (Appendix D).

The four characteristic parameters are highly correlated with elevation, slope, temperature and soil sand content and the environmental variables with latitudinal zonality. This verifies the inference of the distribution law of characteristic parameters previously mentioned. The Di_1, Di_2 and Di_3 values characterising drought tolerance are positively correlated with elevation, slope and temperature, and negatively correlated with soil sandy content, while the CLr value characterising the comprehensive vulnerability is the opposite. The H-H-H loss-type areas with high vulnerability have typical characteristics of low elevation, slope, temperature and high soil sandy content.

From the perspective of an influencing mechanism, when the soil sandy content is high, the soil drainage ability is high, and the crop is more vulnerable to drought, exhibiting low Di_1, Di_2, and Di_3 values and a high CLr value in the vulnerability curve (Reid et al., 2006;Papathoma-Köhle, 2016). The cause-effect relationship between the temperature and the characteristic parameters cannot be defined, although the spatial distributions of the two have a certain correlation. Because temperature stress is removed from the drought scenarios, the temperature variable has no direct influence on the results of yield loss rate to drought and the characteristic parameters. It may have an indirect influence by affecting the crop parameters of winter wheat during the previous calibration process. Similarly, elevation does not directly affect the values of the characteristic parameters. Simulation experiments based on the EPIC model found that changing the input of elevation has little effect on the simulated yield (Thomson et al., 2002). Thus, the elevation may indirectly affect yield and drought vulnerability by acting on other environmental variables such as temperature, precipitation and soil. The aforementioned can provide ideas for the study of the impact of the environment on vulnerability.

Table 3: Correlation between vulnerability characteristic parameters and environmental variables （P≤0.01）

	Di_1	Di_m	Di_2	CLr
Elevation	0.40	0.43	0.37	-0.44

https://doi.org/10.5194/nhess-2019-175
Preprint. Discussion started: 12 August 2019

Slope	0.31	0.44	0.45	-0.48
Soil sand content	-0.10	-0.35	-0.44	0.38
Average temperature during growth period	0.32	0.34	0.30	-0.38
Precipitation during growth period	-0.09	0.19	0.33	-0.26
Relative humidity during growth period	0.41	0.23	0.09	-0.27

4.2 Application of vulnerability curve

By analysing the characteristic parameters distribution, it is found that the winter wheat vulnerability in Europe is lower to the south, particularly in the surrounding areas of the Mediterranean, which is consistent with Mäkinen's findings based on experimental data on wheat varieties (Mäkinen et al., 2018). In addition to reflecting the spatial differences in vulnerability, the characteristic information can accurately express the response feature to drought in various regions and more effectively guide drought risk management. In southern Europe (mainly the L-L-L and L-L-M loss-type vulnerability curves), there is a strong tolerance to mild drought with a Di_1 greater than 0.4, and we should pay more attention to moderate and severe drought reduction. In most of the central region (mainly M-M-M and H-H-H loss-type vulnerability curves), there is a low tolerance to varying degrees to drought, and we should pay attention to the construction of fortification capacity. In the north-eastern region (the L-M-H vulnerability curve), there is susceptibility to droughts with a Di ranging from 0.3 to 0.6, which is a critical stage for drought mitigation. In addition, in regions with H-H-H and L-M-H loss-type vulnerability curves, the Lr relatively slowly increases when the Di is greater than 0.6. At this time, the cost of engineering mitigation means is high and non-engineering means can be considered.

The extent to which climate change affects crop yield depends not only on the temporal and spatial patterns of climate change but also on species characteristics (Trnka et al., 2014;Semenov et al., 2014). The vulnerability curve based on the crop growth process simulation helps to understand the risk from a vulnerability perspective. From the perspective of climate change, precipitation will decrease and evaporation will increase in southern Europe in the future, and drought risk is more likely to increase compared to that of other regions of Europe (IPCC, 2012;Olesen et al., 2011). However, it was found that under the RCP4.5 scenario and using the HadGEM2-ES and MPI-ESM-MR model data for simulation, the drought effects increase in the southern region will be less than or near those of the central and north-eastern regions (Webber et al., 2018), which may be related to a lower vulnerability.

5 Conclusion

Quantitative crop-drought vulnerability assessment and analysis are an important basis for drought risk assessment and drought risk management. Taking European winter wheat as an example, we generate series data of water stress and scenario yield based on EPIC model simulation and then construct S-type drought vulnerability curves. Through characteristic parameters analysis and clustering analysis of vulnerability curves, the loss extent and loss variation characteristics are mapped to identify the regional vulnerability pattern and drought response characteristics. The results provide quantitative ideas for the study of the impact of the environment on vulnerability and provide scientific guidance for regional drought- mitigation resource allocation and strategy development.

https://doi.org/10.5194/nhess-2019-175
Preprint. Discussion started: 12 August 2019

Natural Hazards and Earth System Sciences
Discussions

The winter wheat drought vulnerability in Europe is higher in the south and lower in the north with a latitudinal zonality, which may be related to environmental variables such as elevation, slope, average temperature during growth period and soil sand content. In the southern region, the values of the key points' drought index are high, and the cumulative loss rate is low, indicating a low vulnerability, while the northern region shows the opposite.

The vulnerability curves can be divided into five loss types: Low-Low-Low (L-L-L), Low-Low-Medium (L-L-M), Medium-Medium-Medium (M-M-M), High-High-High (H-H-H) and Low-Medium-High (L-M-H). It is recommended to improve the ability to address drought with a greater than 0.4 intensity in the L-L-L or L-L-M loss-type areas and a drought range from 0.3-0.6 intensity in the L-M-H loss-type areas, as well as improve the ability for drought prevention and mitigation in the M-M-M or H-H-H loss-type areas.

Data availability

The sources of raw data can be found in section 2.2. The code is written for MATLAB, which is available upon request by contacting Yanshen Wu (wuyanshen1012@mail.bnu.edu.cn).

Appendices

Appendix A: Examples of European winter wheat grid vulnerability curves to drought

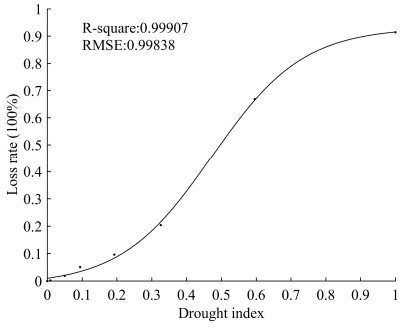

France (grid centre: 1.75° E, 49.25° N)

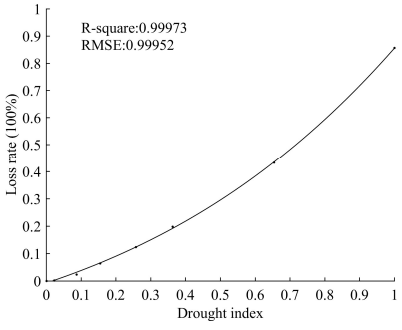

United Kingdom (grid centre: 2.25° W, 53.75° N)

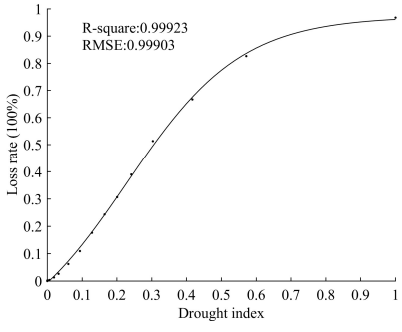

Germany (grid centre: 9.75° E, 54.25° N)

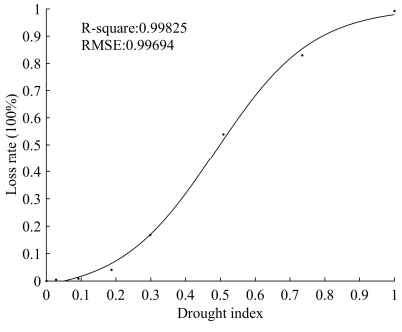

Ukraine (grid centre: 33.25°E, 47.75°N)

https://doi.org/10.5194/nhess-2019-175
Preprint. Discussion started: 12 August 2019

Natural Hazards and Earth System Sciences
Discussions

Appendix B: Clustering effect of different cluster quantities

Quantity of cluster	Quantity of vulnerability curves in each cluster							Within-cluster sum of squared errors (SSE)
	Cluster 1	Cluster 2	Cluster 3	Cluster 4	Cluster 5	Cluster 6	Cluster 7	
3	235	1082	707	-	-	-	-	3711.9
4	257	641	891	235	-	-	-	3340.2
5	475	409	692	245	203	-	-	2794.3
6	3	474	688	410	245	204	-	2538.0
7	3	156	711	157	195	256	546	2519.9

Appendix C: Classificatory key points and cumulative loss rates calculated by category vulnerability curves

Category vulnerability curve	Di_1	Lr_1	Di_2	Lr_2	Di_3	Lr_3	CLr
L-L-L	0.44	0.19	0.67	0.48	0.90	0.76	0.33
L-L-M	0.40	0.19	0.55	0.46	0.69	0.73	0.42
M-M-M	0.28	0.18	0.47	0.47	0.65	0.75	0.50
H-H-H	0.19	0.15	0.38	0.45	0.57	0.76	0.57
L-M-H	0.33	0.19	0.44	0.47	0.56	0.75	0.53
Europe	0.27	0.17	0.47	0.46	0.68	0.75	0.48

Appendix D: Descriptive statistics of environmental variables in various loss-type regions

		L-L-L	L-L-M	M-M-M	H-H-H	L-M-H	Regional
Elevation (m)	Median	677	315	165	140	160	181
	Interquartile Range	636	468	154	125	103	241
Slope (°)	Median	23	12	6	3	3	6
	Interquartile Range	25	17	9	3	3	9
Soil sand content (%)	Median	43	43	43	52	52	43
	Interquartile Range	4	10	22	9	0	12
Precipitation during growth period (mm)	Median	960	646	599	599	638	629
	Interquartile Range	306	198	128	131	53	158
Average temperature during growth period (℃)	Median	7.1	7.8	7.5	6.9	3.9	7.1
	Interquartile Range	3.5	3.6	2.1	1.9	1.1	2.9
Relative humidity during growth period (%)	Median	79.9	80.6	77.5	77.1	80.2	78.8
	Interquartile Range	2.7	3	3.9	3.1	2.1	3.9

https://doi.org/10.5194/nhess-2019-175
Preprint. Discussion started: 12 August 2019

Author contribution

Jing'ai Wang proposed overarching idea and formulated overarching research goals and aims. Hao Guo implemented EPIC model calibration, simulation and vulnerability curves construction. Yanshen Wu and Anyu Zhang developed the vulnerability curves characteristics analysis methods and carried them out. Yanshen Wu drafted and revised manuscript with contributions from all co-authors.

Competing interests

The authors declare that they have no conflict of interest.

Acknowledgements

The National Key Research and Development Program (No. 2016YFA0602402) and the National Basic Research Program of China (No. 2012CB955403) financially supported this research.

References

Barros, I. d., Williams, J. R., and Gaiser, T.: Modeling soil nutrient limitations to crop production in semiarid NE of Brazil with a modified EPIC version: II: Field test of the model, Ecological Modelling, 181, 567-580,doi:https://doi.org/10.1016/j.ecolmodel.2004.03.018, 2005.

Batjes, N. H.: ISRIC-WISE derived soil properties on a 5 by 5 arc-minutes global grid (ver. 1.2), ISRIC - World Soil Information, Wageningen, 2012.

Challinor, A. J., Ewert, F., Arnold, S., Simelton, E., and Fraser, E.: Crops and climate change: progress, trends, and challenges in simulating impacts and informing adaptation, Journal of experimental botany, 60, 2775-2789,doi:10.1093/jxb/erp062, 2009.

Chen, M., Ma, J., Hu, Y., Zhou, F., Li, J., and Yan, L.: Is the S-shaped curve a general law? An application to evaluate the damage resulting from water-induced disasters, Natural Hazards, 78, 497-515,doi:10.1007/s11069-015-1723-9, 2015.

González Tánago, I., Urquijo, J., Blauhut, V., Villarroya, F., and De Stefano, L.: Learning from experience: a systematic review of assessments of vulnerability to drought, Natural Hazards, 80, 951-973,doi:10.1007/s11069-015-2006-1, 2015.

Gottschalk, P. G., and Dunn, J. R.: The five-parameter logistic: a characterization and comparison with the four-parameter logistic, Analytical biochemistry, 343, 54-65,doi:10.1016/j.ab.2005.04.035, 2005.

Guo, H., Zhang, X., Lian, F., Gao, Y., Lin, D., and Wang, J. a.: Drought Risk Assessment Based on Vulnerability Surfaces: A Case Study of Maize, Sustainability, 8, 813,doi:10.3390/su8080813, 2016.

Hempel, S., Frieler, K., Warszawski, L., Schewe, J., and Piontek, F.: A trend-preserving bias correction – the ISI-MIP approach, Earth Syst. Dynam., 4, 219-236,doi:10.5194/esd-4-219-2013, 2013.

Hu, L., Tian, K., Wang, X., and Zhang, J.: The "S" curve relationship between export diversity and economic size of countries, Physica A: Statistical Mechanics and its Applications, 391, 731-739,doi:10.1016/j.physa.2011.08.048, 2012.

Huang, J., Liu, Y., Ma, L., and Su, F.: Methodology for the assessment and classification of regional

https://doi.org/10.5194/nhess-2019-175
Preprint. Discussion started: 12 August 2019

vulnerability to natural hazards in China: the application of a DEA model, Natural Hazards, 65, 115-134,doi:10.1007/s11069-012-0348-5, 2012.

IPCC: Summary for Policymakers. In: Managing the Risks of Extreme Events and Disasters to Advance Climate Change Adaptation. A Special Report of Working Groups I and II of the Intergovernmental Panel on Climate Change. Cambridge University Press, Cambridge, UK, and New York, NY, USA, pp. 1-19., edited by: [Field, C. B., V. Barros, T.F. Stocker, D. Qin, D.J. Dokken, K.L. Ebi, M.D. Mastrandrea, K.J. Mach, G.-K. Plattner, S.K. Allen, M. Tignor, and P.M. Midgley (eds.)], 2012.

IPCC: Climate Change 2014: Synthesis Report, Contribution of Working Groups I, II and III to the Fifth Assessment Report of the Intergovernmental Panel on Climate Change, edited by: Core Writing Team, R. K. P. a. L. A. M., IPCC, Geneva, Switzerland, 2014.

J, W. J., P, G. G., K, Z. H., H, L. J., F, W. Q., and H, Y. J.: Global vulnerability to agricultural drought and its spatial characteristics, Science China Earth Sciences, 60, 910-920,doi:10.1007/s11430-016-9018-2, 2017.

Jacques, J., and Preda, C.: Functional data clustering: a survey, Advances in Data Analysis and Classification, 8, 231-255,doi:10.1007/s11634-013-0158-y, 2014.

Jain, V. K., Pandey, R. P., and Jain, M. K.: Spatio-temporal assessment of vulnerability to drought, Natural Hazards, 76, 443-469,doi:10.1007/s11069-014-1502-z, 2014.

James, G. M., and Sugar, C. A.: Clustering for Sparsely Sampled Functional Data, Journal of the American Statistical Association, 98, 397-408,doi:10.1198/016214503000189, 2003.

Jayanthi, H., Husak, G. J., Funk, C., Magadzire, T., Adoum, A., and Verdin, J. P.: A probabilistic approach to assess agricultural drought risk to maize in Southern Africa and millet in Western Sahel using satellite estimated rainfall, International Journal of Disaster Risk Reduction, 10, 490-502,doi:10.1016/j.ijdrr.2014.04.002, 2014.

Jianjun, W., Bin, H., Aifeng, L., Lei, Z., Ming, L., and Lin, Z.: Quantitative assessment and spatial characteristics analysis of agricultural drought vulnerability in China, Natural Hazards, 56, 785-801,doi:10.1007/s11069-010-9591-9, 2010.

Knutson C, H. M., Phillips T: How to reduce drought risk, preparedness and mitigation working group of the western drought coordination council, Lincoln, Nebraska, 1998.

Kogan, F. N.: Global Drought Watch from Space, Bulletin of the American Meteorological Society, 78, 621–636, 1997.

Kucharavy, D., and De Guio, R.: Application of S-shaped curves, Procedia Engineering, 9, 559-572,doi:10.1016/j.proeng.2011.03.142, 2011.

Lantican, M. A., H.J. Dubin, and Morris, M. L.: Impacts of international wheat breeding research in the developing world, 1988-2002, Mexico, D.F.: CIMMYT, 2005.

Li, Y., Ye, W., Wang, M., and Yan, X.: Climate change and drought: a risk assessment of crop-yield impacts, Climate Research, 39, 31-46,doi:10.3354/cr00797, 2009.

Mäkinen, H., Kaseva, J., Trnka, M., Balek, J., Kersebaum, K. C., Nendel, C., Gobin, A., Olesen, J. E., Bindi, M., Ferrise, R., Moriondo, M., Rodríguez, A., Ruiz-Ramos, M., Takáč, J., Bezák, P., Ventrella, D., Ruget, F., Capellades, G., and Kahiluoto, H.: Sensitivity of European wheat to extreme weather, Field Crops Research, 222, 209-217,doi:10.1016/j.fcr.2017.11.008, 2018.

https://doi.org/10.5194/nhess-2019-175
Preprint. Discussion started: 12 August 2019

Mishra, A. K., and Singh, V. P.: A review of drought concepts, Journal of Hydrology, 391, 202-216,doi:10.1016/j.jhydrol.2010.07.012, 2010.

Monfreda, C., Ramankutty, N., and Foley, J. A.: Farming the planet: 2. Geographic distribution of crop areas, yields, physiological types, and net primary production in the year 2000, Global Biogeochemical Cycles, 22,doi:10.1029/2007gb002947, 2008.

Food and Agriculture Organization of the United Nations, and International Institute for Applied Systems Analysis.: Median of terrain slopes derived from GTOPO30, Global Agro-ecological Zones, http://www.iiasa.ac.at/Research/LUC/GAEZ/index.htm, 2000.

Oki, T.: Argicultural Withdrawal 3 - based on Dr. Tan's EPIC (Real and Maximum) : Version 1, OKI Laboratory, University of Tokyo, http://hydro.iis.u-tokyo.ac.jp/GW/result/global/annual/withdrawal/index.html, 2002.

Olesen, J. E., Trnka, M., Kersebaum, K. C., Skjelvåg, A. O., Seguin, B., Peltonen-Sainio, P., Rossi, F., Kozyra, J., and Micale, F.: Impacts and adaptation of European crop production systems to climate change, European Journal of Agronomy, 34, 96-112,doi:10.1016/j.eja.2010.11.003, 2011.

Palosuo, T., Kersebaum, K. C., Angulo, C., Hlavinka, P., Moriondo, M., Olesen, J. E., Patil, R. H., Ruget, F., Rumbaur, C., Takáč, J., Trnka, M., Bindi, M., Çaldağ, B., Ewert, F., Ferrise, R., Mirschel, W., Şaylan, L., Šiška, B., and Rötter, R.: Simulation of winter wheat yield and its variability in different climates of Europe: A comparison of eight crop growth models, European Journal of Agronomy, 35, 103-114,doi:10.1016/j.eja.2011.05.001, 2011.

Pandey, R. P., Pandey, A., Galkate, R. V., Byun, H.-R., and Mal, B. C.: Integrating Hydro-Meteorological and Physiographic Factors for Assessment of Vulnerability to Drought, Water Resources Management, 24, 4199-4217,doi:10.1007/s11269-010-9653-5, 2010.

Papathoma-Köhle, M.: Vulnerability curves vs. vulnerability indicators: application of an indicator-based methodology for debris-flow hazards, Natural Hazards and Earth System Sciences, 16, 1771-1790,doi:10.5194/nhess-16-1771-2016, 2016.

Potter, P., Ramankutty, N., Bennett, E. M., and Donner, S. D.: Characterizing the Spatial Patterns of Global Fertilizer Application and Manure Production, Earth Interactions, 14, 1-22,doi:10.1175/2009ei288.1, 2010.

Reid, S., Smit, B., Caldwell, W., and Belliveau, S.: Vulnerability and adaptation to climate risks in Ontario agriculture, Mitigation and Adaptation Strategies for Global Change, 12, 609-637,doi:10.1007/s11027-006-9051-8, 2006.

Sacks, W. J., Deryng, D., Foley, J. A., and Ramankutty, N.: Crop planting dates: an analysis of global patterns, Global Ecology and Biogeography, 19, 607-620,doi:10.1111/j.1466-8238.2010.00551.x, 2010.

Semenov, M. A., Stratonovitch, P., Alghabari, F., and Gooding, M. J.: Adapting wheat in Europe for climate change, Journal of cereal science, 59, 245-256,doi:10.1016/j.jcs.2014.01.006, 2014.

Simelton, E., Fraser, E. D. G., Termansen, M., Forster, P. M., and Dougill, A. J.: Typologies of crop-drought vulnerability: an empirical analysis of the socio-economic factors that influence the sensitivity and resilience to drought of three major food crops in China (1961–2001), Environmental Science & Policy, 12, 438-452,doi:10.1016/j.envsci.2008.11.005, 2009.

United States Geological Survey .: Global 30 Arc-Second Elevation

https://doi.org/10.5194/nhess-2019-175
Preprint. Discussion started: 12 August 2019

(GTOPO30),doi:/10.5066/F7DF6PQS, 1996.

, A. M., Brown, R. A., Ghan, S. J., Izaurralde, R. C., Rosenberg, N. J., and Leung, L. R.: Elevation Dependence of Winter Wheat Production in Eastern Washington State with Climate Change: A Methodological Study, Climatic Change, 54, 141-164,doi:10.1023/a:1015743411557, 2002.

Todisco, F., Mannocchi, F., and Vergni, L.: Severity–duration–frequency curves in the mitigation of drought impact: an agricultural case study, Natural Hazards, 65, 1863-1881,doi:10.1007/s11069-012-0446-4, 2012.

Trnka, M., Rötter, R. P., Ruiz-Ramos, M., Kersebaum, K. C., Olesen, J. E., Žalud, Z., and Semenov, M. A.: Adverse weather conditions for European wheat production will become more frequent with climate change, Nature Climate Change, 4, 637,doi:10.1038/nclimate2242, 2014.

Wang, X. C., and Li, J.: Evaluation of crop yield and soil water estimates using the EPIC model for the Loess Plateau of China, Mathematical and Computer Modelling, 51, 1390-1397,doi:https://doi.org/10.1016/j.mcm.2009.10.030, 2010.

Wang, X. C., Li, J., Tahir, M. N., and Hao, M. D.: Validation of the EPIC model using a long-term experimental data on the semi-arid Loess Plateau of China, Mathematical and Computer Modelling, 54, 976-986,doi:https://doi.org/10.1016/j.mcm.2010.11.025, 2011.

Wang, Z., He, F., Fang, W., and Liao, Y.: Assessment of physical vulnerability to agricultural drought in China, Natural Hazards, 67, 645-657,doi:10.1007/s11069-013-0594-1, 2013.

Webber, H., Ewert, F., Olesen, J. E., Muller, C., Fronzek, S., Ruane, A. C., Bourgault, M., Martre, P., Ababaei, B., Bindi, M., Ferrise, R., Finger, R., Fodor, N., Gabaldon-Leal, C., Gaiser, T., Jabloun, M., Kersebaum, K. C., Lizaso, J. I., Lorite, I. J., Manceau, L., Moriondo, M., Nendel, C., Rodriguez, A., Ruiz-Ramos, M., Semenov, M. A., Siebert, S., Stella, T., Stratonovitch, P., Trombi, G., and Wallach, D.: Diverging importance of drought stress for maize and winter wheat in Europe, Nature communications, 9, 4249,doi:10.1038/s41467-018-06525-2, 2018.

Wilhelmi, O. V., and Wilhite, D. A.: Assessing Vulnerability to Agricultural Drought: A Nebraska Case Study, Natural Hazards, 25, 37-58,doi:10.1023/a:1013388814894, 2002.

Williams, J., Jones, C., and Dyke, P.: The EPIC model and its application, In Proc. Int. Symp. on minimum data sets for agrotechnology transfer, 1984, 111-121,

Xingming, Z., Chunqin, Z., Hao, G., Weixia, Y., Ran, W., and Jing'ai, W.: Drought risk assessment on world wheat based on grid vulnerability curves, Journal of Catastrophology, 30, 228-234,doi:10. 3969 /j. issn. 1000－811X. 2015. 02. 042, 2015.

Yao, Z., and Jing'ai, W.: A review on development of vulnerability curve of natural disaster, Advances in Earth Science, 27, 435-442,doi:10.11867/j.issn.1001-8166.2012.04.0435, 2012.

Yuan-yuan, Y., Jing-ai1, W., Xiao-yun, H., and Yong-deng, L.: Progress of Indices and Models of Drought Risk Assessment at Global Scale, ARID ZONE RESEARCH, 31, 619-626,doi:10.13866 /j.azr. 2014.04.06, 2014.

Yue, Y., Li, J., Ye, X., Wang, Z., Zhu, A. X., and Wang, J.-a.: An EPIC model-based vulnerability assessment of wheat subject to drought, Natural Hazards, 78, 1629-1652,doi:10.1007/s11069-015-1793-8, 2015.

Zhi-qiang, W., Wei-hua, F., Fei, H., and Hon, X.: Effect of climate change on wheat yield in northern

https://doi.org/10.5194/nhess-2019-175
Preprint. Discussion started: 12 August 2019

Natural Hazards and Earth System Sciences
Discussions

China: a research based on EPIC model, JOURNAL OF NATURAL DISASTERS, 17, 109-114,doi:10.13577/j .jnd.2008.0119, 2008.